

# Minnaert resonances for acoustic waves in bubbly media<sup>\*</sup>

Habib Ammari<sup>†</sup>      Brian Fitzpatrick<sup>†</sup>      David Gontier<sup>†</sup>      Hyundae Lee<sup>‡</sup>  
Hai Zhang<sup>§</sup>

## Abstract

Through the application of layer potential techniques and Gohberg-Sigal theory we derive an original formula for the Minnaert resonance frequencies of arbitrarily shaped bubbles. We also provide a mathematical justification for the monopole approximation of scattering of acoustic waves by bubbles at their Minnaert resonant frequency. Our results are complemented by several numerical examples which serve to validate our formula in two dimensions.

Mathematics Subject Classification (MSC2000): 35R30, 35C20.

Keywords: Minnaert resonance, bubble, monopole approximation, layer potentials, acoustic waves.

## 1 Introduction

The purpose of this work is to understand acoustic wave propagation through a liquid containing bubbles. Our motivation is the use of bubbles in medical ultrasonic imaging as strong sound scatterers at particular frequencies known as Minnaert resonances [21]. Many interesting physical works have been devoted to the acoustic bubble problem [8, 10, 13, 15, 18, 19]. Nevertheless, the characterization of the Minnaert resonances for arbitrary shaped bubbles has been a longstanding problem.

In this paper we derive an original formula for the Minnaert resonances of bubbles of arbitrary shapes using layer potential techniques and Gohberg-Sigal theory [14, 2]. Our formula can be generalized to multiple bubbles. We provide a mathematical justification for the monopole approximation and demonstrate the enhancement of the scattering in the far field at the Minnaert resonance. We show that there is a correspondence between bubbles in water and plasmonic nanoparticles in that both raise similar fundamental questions [3]. However, the mathematical formulation of Minnaert resonances is much more involved than the formulation of plasmonic resonances.

The Minnaert resonance is a low frequency resonance in which the wavelength is much larger than the size of the bubble [10, 21]. Our results in this paper have important applications. They

---

<sup>\*</sup>This work was supported by the ERC Advanced Grant Project MULTIMOD-267184. Hyundae Lee was supported by NRF-2015R1D1A1A01059357 grant. Hai Zhang was supported by a startup fund from HKUST.

<sup>†</sup>Department of Mathematics, ETH Zürich, Rämistrasse 101, CH-8092 Zürich, Switzerland (habib.ammari@math.ethz.ch, brian.fitzpatrick@sam.math.ethz.ch, david.gontier@sam.math.ethz.ch).

<sup>‡</sup>Department of Mathematics, Inha University, 253 Yonghyun-dong Nam-gu, Incheon 402-751, Korea (hdlee@inha.ac.kr).

<sup>§</sup>Department of Mathematics, HKUST, Clear Water Bay, Kowloon, Hong Kong (haizhang@ust.hk).

can be used to show that at the Minnaert resonance it is possible to achieve superfocusing of acoustic waves or imaging of passive sources with a resolution beyond the Rayleigh diffraction limit [4, 5]. Foldy's approximation applies and yields to the conclusion that the medium surrounding the source behaves like a high contrast dispersive medium [12]. As the dispersion is small, it has little effect on the superfocusing and superresolution phenomena. Effective equations for wave propagation in bubbly liquids have been derived in the low frequency regime where the frequency is much smaller than the Minnaert resonance frequency [6, 7, 16]. In this paper, however, we are more concerned with wave propagation in the resonant regime.

The paper is organized as follows. In Section 2 we consider the scattering of acoustic waves in three dimensions by a single bubble and derive its Minnaert resonances in terms of its capacity, volume, and material parameters. In Section 3 we derive the point scatterer approximation of the bubble in the far-field. In Section 4 we perform numerical simulations in two dimensions to illustrate the main findings of this paper. The paper ends with some concluding remarks. In Appendix A, we collect some useful asymptotic formulas for layer potentials in two and three dimensions. Derivations of the two-dimensional Minnaert resonances are given in Appendix B.

## 2 The Minnaert resonance

We consider the scattering of acoustic waves in a homogeneous media by a bubble embedded inside. Assume that the bubble occupies a bounded and simply connected domain  $D$  with  $\partial D \in C^{1,s}$  for some  $0 < s < 1$ . We denote by  $\rho_b$  and  $\kappa_b$  the density and the bulk modulus of the air inside the bubble, respectively, and by  $\rho$  and  $\kappa$  the corresponding parameters for the background media  $\mathbb{R}^3 \setminus D$ . The scattering problem can be modeled by the following equations:

$$\left\{ \begin{array}{l} \nabla \cdot \frac{1}{\rho} \nabla u + \frac{\omega^2}{\kappa} u = 0 \quad \text{in } \mathbb{R}^3 \setminus D, \\ \nabla \cdot \frac{1}{\rho_b} \nabla u + \frac{\omega^2}{\kappa_b} u = 0 \quad \text{in } D, \\ u_+ - u_- = 0 \quad \text{on } \partial D, \\ \frac{1}{\rho} \frac{\partial u}{\partial \nu} \Big|_+ - \frac{1}{\rho_b} \frac{\partial u}{\partial \nu} \Big|_- = 0 \quad \text{on } \partial D, \\ u^s := u - u^i \text{ satisfies the Sommerfeld radiation condition.} \end{array} \right. \quad (2.1)$$

Here,  $\partial/\partial \nu$  denotes the outward normal derivative and  $|_{\pm}$  denote the limits from outside and inside  $D$ .

We introduce some parameters to facilitate our analysis. We let

$$v = \sqrt{\frac{\kappa}{\rho}}, \quad v_b = \sqrt{\frac{\kappa_b}{\rho_b}}, \quad k = \frac{\omega}{v} \quad \text{and} \quad k_b = \frac{\omega}{v_b}$$

be respectively the speed of sound outside and inside the bubble, and the wave-number outside and inside the bubble. We also introduce two dimensionless contrast parameters

$$\delta = \frac{\rho_b}{\rho} \quad \text{and} \quad \tau = \frac{k_b}{k} = \frac{v}{v_b} = \sqrt{\frac{\rho_b \kappa}{\rho \kappa_b}}.$$

By choosing proper physical units, we may assume that the size of the bubble is of order 1 and that the wave speeds outside and inside the bubble are both of order 1. Thus the contrast between the wave speeds is not significant. We assume, however, that there is a large contrast in the bulk moduli. In summary, we assume that  $\delta \ll 1$  and  $\tau = O(1)$ .

We use layer potentials to represent the solution to the scattering problem (2.1). Let the single layer potential  $\mathcal{S}_D^k : L^2(\partial D) \rightarrow H^1(\partial D), H_{\text{loc}}^1(\mathbb{R}^3)$  associated with  $D$  and wavenumber  $k$  be defined by

$$\forall \mathbf{x} \in \mathbb{R}^3, \quad \mathcal{S}_D^k[\psi](\mathbf{x}) := \int_{\partial D} G_k(\mathbf{x}, \mathbf{y}) \psi(\mathbf{y}) d\sigma(\mathbf{y}),$$

where

$$G_k(\mathbf{x}, \mathbf{y}) := -\frac{e^{ik|\mathbf{x}-\mathbf{y}|}}{4\pi|\mathbf{x}-\mathbf{y}|}$$

is the Green function of the Helmholtz equation in  $\mathbb{R}^3$ , subject to the Sommerfeld radiation condition. We also define the boundary integral operator  $\mathcal{K}_D^{k,*} : L^2(\partial D) \rightarrow L^2(\partial D)$  by

$$\forall \mathbf{x} \in D, \quad \mathcal{K}_D^{k,*}[\psi](\mathbf{x}) := \int_{\partial D} \frac{\partial G_k(\mathbf{x}, \mathbf{y})}{\partial \nu(\mathbf{x})} \psi(\mathbf{y}) d\sigma(\mathbf{y}).$$

We then look for a solution  $u$  of (2.1) of the form

$$u = \begin{cases} u^{\text{in}} + \mathcal{S}_D^k[\psi], & \text{on } \mathbb{R}^3 \setminus \bar{D}, \\ \mathcal{S}_D^{k_b}[\psi_b], & \text{on } D, \end{cases} \quad (2.2)$$

for some surface potentials  $\psi, \psi_b \in L^2(\partial D)$ . Using the jump relations for the single layer potentials [2], one can show that (2.1) is equivalent to the boundary integral equation

$$\mathcal{A}(\omega, \delta)[\Psi] = F, \quad (2.3)$$

where

$$\mathcal{A}(\omega, \delta) = \begin{pmatrix} \mathcal{S}_D^{k_b} & -\mathcal{S}_D^k \\ -\frac{1}{2} + \mathcal{K}_D^{k_b,*} & -\delta(\frac{1}{2} + \mathcal{K}_D^{k,*}) \end{pmatrix}, \quad \Psi = \begin{pmatrix} \psi_b \\ \psi \end{pmatrix}, \quad F = \begin{pmatrix} u^{\text{in}} \\ \delta \frac{\partial u^{\text{in}}}{\partial \nu} \end{pmatrix}.$$

Throughout the paper, we denote by  $\mathcal{H} = L^2(\partial D) \times L^2(\partial D)$  and by  $\mathcal{H}_1 = H^1(\partial D) \times L^2(\partial D)$ , and use  $(\cdot, \cdot)$  for the inner product in  $L^2$  spaces and  $\|\cdot\|_{\mathcal{H}}$  for the norm in  $\mathcal{H}$ . Here,  $H^1(\partial D)$  is the standard Sobolev space. It is clear that  $\mathcal{A}(\omega, \delta)$  is a bounded linear operator from  $\mathcal{H}$  to  $\mathcal{H}_1$ , *i.e.*  $\mathcal{A}(\omega, \delta) \in \mathcal{B}(\mathcal{H}, \mathcal{H}_1)$ .

We define the resonances of the bubble in the scattering problem (2.1) as the complex numbers  $\omega$  with negative imaginary part such that there exists a nontrivial solution to

$$\mathcal{A}(\omega, \delta)[\Psi] = 0. \quad (2.4)$$

These can be viewed as the characteristic values of the operator-valued analytic function  $\omega \mapsto \mathcal{A}(\omega, \delta)$ . We are interested in the quasi-static resonances of the bubble, or the resonance frequencies for which the size of the bubble is much smaller than the wavelength  $2\pi k^{-1}$ . In some physics literature, this resonance is called the *Minnaert resonance* [21]. Due to our assumptions on the bubble being of size order 1, and the wave speed outside of the bubble also being of order 1, this resonance should lie in a small neighborhood of the origin in the complex plane. In what

follows, we apply the Gohberg-Sigal theory to find this resonance.

We first look at the limiting case when  $\delta = \omega = 0$ . We set for clarity  $\mathcal{S}_D := \mathcal{S}_D^{k=0}$ ,  $\mathcal{K}_D^* := \mathcal{K}_D^{k=0,*}$ , and we define

$$\mathcal{A}_0 := \mathcal{A}(0, 0) = \begin{pmatrix} \mathcal{S}_D & -\mathcal{S}_D \\ -\frac{1}{2} + \mathcal{K}_D^* & 0 \end{pmatrix}. \quad (2.5)$$

We denote by  $\mathbb{1}_{\partial D} \in H^1(\partial D)$  the constant function on  $\partial D$  with value 1, and by  $\mathcal{A}_0^* : \mathcal{H}_1 \rightarrow \mathcal{H}$  the adjoint of  $\mathcal{A}_0$ . We recall that  $\text{Ker}(\mathcal{K}_D^* - \frac{1}{2}) = \text{Vect}\{\psi_0\}$ , for some  $\psi_0 \in \mathcal{H}$ . We choose the normalization of  $\psi_0$  so that  $(\mathbb{1}_{\partial D}, \psi_0) = \int_{\partial D} \psi_0 = 1$ . With this normalization, it holds that  $\mathcal{S}_D[\psi_0] = -\text{Cap}_D^{-1} \mathbb{1}_{\partial D}$ , where  $\text{Cap}_D$  is the capacity of the set  $D$ .

**Lemma 2.1.** *It holds that  $\text{Ker}(\mathcal{A}_0) = \text{Vect}\{\Psi_0\}$  and that  $\text{Ker}(\mathcal{A}_0^*) = \text{Vect}\{\Phi_0\}$ , where we set*

$$\Psi_0 = \begin{pmatrix} \psi_0 \\ \psi_0 \end{pmatrix} \quad \text{and} \quad \Phi_0 = \begin{pmatrix} 0 \\ \mathbb{1}_{\partial D} \end{pmatrix}.$$

The above lemma shows that  $\omega = 0$  is a characteristic value for the operator-valued analytic function  $\mathcal{A}(\omega, \delta)$ . By the Gohberg-Sigal theory [2, 14], we can conclude the following result about the existence of the quasi-static resonance.

**Lemma 2.2.** *For any  $\delta$  sufficiently small, there exists a characteristic value  $\omega_0 = \omega_0(\delta)$  to the operator-valued analytic function  $\mathcal{A}(\omega, \delta)$  such that  $\omega_0(0) = 0$  and  $\omega_0$  depends on  $\delta$  continuously.*

By performing the asymptotic analysis of the operator  $\mathcal{A}(\omega, \delta)$ , we are able to calculate the first orders of  $\delta \mapsto \omega_0(\delta)$ . Our main result in this section is stated in the following theorem.

**Theorem 2.1.** *In the quasi-static regime, there exist two resonances for a single bubble, of the form ( $|D|$  denotes the volume of  $D$ ).*

$$\omega_{\pm}(\delta) = \pm \left( \sqrt{\frac{\text{Cap}_D v_b^2}{|D|}} \right) \delta^{\frac{1}{2}} - i \left( \frac{\text{Cap}_D^2 v_b^2}{8\pi v |D|} \right) \delta + O(\delta^{\frac{3}{2}}).$$

The resonance  $\omega_+$  is what is usually called the *Minnaert resonance*.

**Remark 2.1.** *In the two-dimensional case, we find another expansion. The main differences between the two-dimensional case and the three-dimensional case are explained in Appendix B.*

**Remark 2.2.** *In the case of a collection of  $N$  identical bubbles, with separation distance much larger than their characteristic sizes, the Minnaert resonance for a single bubble will be split into  $N$  resonances. The splitting will be related to the eigenvalues of a  $N$ -by- $N$  matrix which encodes information on the configuration of the  $N$  bubbles. This can be proved by a similar argument as in [4].*

**Remark 2.3.** *In the special case when  $D$  is the sphere of radius  $R$ , we have  $\text{Cap}_D = 4\pi R$  and  $|D| = \frac{4\pi}{3} R^3$ . Consequently, the Minnaert resonance is given by*

$$\omega_+(\delta) = \frac{v_b}{R} \sqrt{3\delta} - i \frac{3v_b^2 \delta}{2Rv}.$$

*The leading term  $\omega_M = \sqrt{3\delta} v_b / R$  was already derived by Minnaert [21].*

*Proof of Theorem 2.1.* We find the resonance by solving

$$\mathcal{A}(\omega, \delta)[\Psi_\delta] = 0. \quad (2.6)$$

• **Asymptotic analysis of  $\mathcal{A}(\omega, \delta)$ .** Let us first study the operator  $\mathcal{A}(\omega, \delta)$ . Using the results in Appendix A, we can derive the following result.

**Lemma 2.3.** *In the space  $\mathcal{B}(\mathcal{H}, \mathcal{H}_1)$ , we have*

$$\mathcal{A}(\omega, \delta) := \mathcal{A}_0 + \mathcal{B}(\omega, \delta) = \mathcal{A}_0 + \omega \mathcal{A}_{1,0} + \omega^2 \mathcal{A}_{2,0} + \omega^3 \mathcal{A}_{3,0} + \delta \mathcal{A}_{0,1} + \delta \omega^2 \mathcal{A}_{2,1} + O(|\omega|^4 + |\delta \omega^3|)$$

where we define

$$\mathcal{A}_{1,0} = \begin{pmatrix} v_b^{-1} \mathcal{S}_{D,1} & -v^{-1} \mathcal{S}_{D,1} \\ 0 & 0 \end{pmatrix}, \quad \mathcal{A}_{2,0} = \begin{pmatrix} v_b^{-2} \mathcal{S}_{D,2} & -v^{-2} \mathcal{S}_{D,2} \\ v_b^{-2} \mathcal{K}_{D,2}^* & 0 \end{pmatrix}, \quad \mathcal{A}_{3,0} = \begin{pmatrix} v_b^{-3} \mathcal{S}_{D,3} & -v^{-3} \mathcal{S}_{D,3} \\ v_b^{-3} \mathcal{K}_{D,3}^* & 0 \end{pmatrix},$$

$$\mathcal{A}_{0,1} = \begin{pmatrix} 0 & 0 \\ 0 & -(\frac{1}{2} + \mathcal{K}_D^*) \end{pmatrix}, \quad \mathcal{A}_{2,1} = \begin{pmatrix} 0 & 0 \\ 0 & -v^{-2} \mathcal{K}_{D,2}^* \end{pmatrix}.$$

We now define a rank-1 operator  $\mathcal{P}_0$  from  $\mathcal{H}$  to  $\mathcal{H}_1$  by  $\mathcal{P}_0[\Psi] := (\Psi, \Psi_0)\Phi_0$ , and denote by  $\tilde{\mathcal{A}}_0 = \mathcal{A}_0 + \mathcal{P}_0$ .

**Lemma 2.4.** *We have*

(i) *The operator  $\tilde{\mathcal{A}}_0$  is a bijective operator in  $\mathcal{B}(\mathcal{H}, \mathcal{H}_1)$ . Moreover,  $\tilde{\mathcal{A}}_0[\Psi_0] = \|\Psi_0\|^2 \Phi_0$ ;*

(ii) *Its adjoint  $\tilde{\mathcal{A}}_0^*$  is a bijective operator in  $\mathcal{B}(\mathcal{H}_1, \mathcal{H})$ . Moreover,  $\tilde{\mathcal{A}}_0^*[\Phi_0] = \|\Phi_0\|^2 \Psi_0$ .*

*Proof.* By construction, and the fact that  $\mathcal{S}_D$  is bijective from  $L^2(\partial D)$  to  $H^1(\partial D)$  [1], we can show that  $\tilde{\mathcal{A}}_0$  (hence  $\tilde{\mathcal{A}}_0^*$ ) is bijective. The fact that  $\tilde{\mathcal{A}}_0[\Psi_0] = 2\|\psi_0\|^2 \Phi_0$  is direct. Finally, by noticing that  $\mathcal{P}_0^*[\theta] = (\theta, \Phi_0)\Psi_0$ , it follows that  $\tilde{\mathcal{A}}_0^*[\Phi_0] = \mathcal{P}_0^*[\Phi_0] = \|\mathbb{1}_{\partial D}\|^2 \Psi_0$ .  $\square$

• **Strategy of the proof.**

Write  $\Psi_\delta = \Psi_0 + \Psi_1$  and assume the orthogonality condition  $(\Psi_1, \Psi_0) = 0$ . Since  $\tilde{\mathcal{A}}_0 = \mathcal{A}_0 + \mathcal{P}_0$ , Equation (2.6) is equivalent to

$$(\tilde{\mathcal{A}}_0 - \mathcal{P}_0 + \mathcal{B})[\Psi_0 + \Psi_1] = 0.$$

Observe that the operator  $\tilde{\mathcal{A}}_0 + \mathcal{B}$  is invertible for sufficiently small  $\delta$  and  $\omega$ . Applying  $(\tilde{\mathcal{A}}_0 + \mathcal{B})^{-1}$  to both sides of the above equation leads to

$$\Psi_1 = (\tilde{\mathcal{A}}_0 + \mathcal{B})^{-1} \mathcal{P}_0[\Psi_0] - \Psi_0 = \|\Psi_0\|^2 (\tilde{\mathcal{A}}_0 + \mathcal{B})^{-1}[\Phi_0] - \Psi_0. \quad (2.7)$$

Using the orthogonality condition, we deduce that (2.6) has a solution if and only if

$$\tilde{A}(\omega, \delta) := \|\Psi_0\|^2 \left( \left( (\tilde{\mathcal{A}}_0 + \mathcal{B})^{-1}[\Phi_0], \Psi_0 \right) - 1 \right) = 0. \quad (2.8)$$

Let us calculate  $A(\omega, \delta) := \tilde{A}(\omega, \delta) \|\Phi_0\|$ . Using the Neumann series

$$(\tilde{\mathcal{A}}_0 + \mathcal{B})^{-1} = \left( 1 + \tilde{\mathcal{A}}_0^{-1} \mathcal{B} \right)^{-1} \tilde{\mathcal{A}}_0^{-1} = \left( 1 - \tilde{\mathcal{A}}_0^{-1} \mathcal{B} + \tilde{\mathcal{A}}_0^{-1} \mathcal{B} \tilde{\mathcal{A}}_0^{-1} \mathcal{B} - \dots \right) \tilde{\mathcal{A}}_0^{-1},$$

and the fact that  $\tilde{\mathcal{A}}_0^{-1}[\Phi_0] = \|\Psi_0\|^{-2} \Psi_0$  and  $\tilde{\mathcal{A}}_0^{-1}[\Psi_0] = \|\Phi_0\|^{-2} \Phi_0$ , we obtain that

$$\begin{aligned} A(\omega, \delta) = & -\omega (\mathcal{A}_{1,0}[\Psi_0], \Phi_0) - \omega^2 (\mathcal{A}_{2,0}[\Psi_0], \Phi_0) - \omega^3 (\mathcal{A}_{3,0}[\Psi_0], \Phi_0) - \delta (\mathcal{A}_{0,1}[\Psi_0], \Phi_0) \\ & + \omega^2 (\mathcal{A}_{1,0} \tilde{\mathcal{A}}_0^{-1} \mathcal{A}_{1,0}[\Psi_0], \Phi_0) + \omega^3 (\mathcal{A}_{1,0} \tilde{\mathcal{A}}_0^{-1} \mathcal{A}_{2,0}[\Psi_0], \Phi_0) + \omega^3 (\mathcal{A}_{2,0} \tilde{\mathcal{A}}_0^{-1} \mathcal{A}_{1,0}[\Psi_0], \Phi_0) \\ & + \omega \delta (\mathcal{A}_{1,0} \tilde{\mathcal{A}}_0^{-1} \mathcal{A}_{0,1}[\Psi_0], \Phi_0) + \omega \delta (\mathcal{A}_{0,1} \tilde{\mathcal{A}}_0^{-1} \mathcal{A}_{1,0}[\Psi_0], \Phi_0) \\ & + \omega^3 (\mathcal{A}_{1,0} \tilde{\mathcal{A}}_0^{-1} \mathcal{A}_{1,0} \tilde{\mathcal{A}}_0^{-1} \mathcal{A}_{1,0}[\Psi_0], \Phi_0) + O(|\omega|^4 + |\delta| |\omega|^2 + |\delta|^2). \end{aligned}$$

It is clear that  $\mathcal{A}_{1,0}^*[\Phi_0] = 0$ . Consequently, the expression simplifies into

$$\begin{aligned} A(\omega, \delta) = & -\omega^2 (\mathcal{A}_{2,0}[\Psi_0], \Phi_0) - \omega^3 (\mathcal{A}_{3,0}[\Psi_0], \Phi_0) + \omega^3 (\mathcal{A}_{2,0} \tilde{\mathcal{A}}_0^{-1} \mathcal{A}_{1,0}[\Psi_0], \Phi_0) \\ & - \delta (\mathcal{A}_{0,1}[\Psi_0], \Phi_0) + \omega \delta (\mathcal{A}_{0,1} \tilde{\mathcal{A}}_0^{-1} \mathcal{A}_{1,0}[\Psi_0], \Phi_0) + O(|\omega|^4 + |\delta| |\omega|^2 + |\delta|^2). \end{aligned} \quad (2.9)$$

We now calculate the five remaining terms.

- **Calculation of  $(\mathcal{A}_{2,0}[\Psi_0], \Phi_0)$ .** Using the first point of Lemma A.1, we get

$$\begin{aligned} (\mathcal{A}_{2,0}[\Psi_0], \Phi_0) &= v_b^{-2} (\mathcal{K}_{D,2}^*[\psi_0], \mathbf{1}_{\partial D}) = v_b^{-2} (\psi_0, \mathcal{K}_{D,2}[\mathbf{1}_{\partial D}]) \\ &= -v_b^{-2} \int_{\partial D} \psi_0(\mathbf{x}) \int_D G_0(\mathbf{x} - \mathbf{y}) d\mathbf{y} d\sigma(\mathbf{x}) = -v_b^{-2} \int_D \mathcal{S}_D[\phi_0](\mathbf{x}) d\mathbf{x} = \frac{|D|}{v_b^2 \text{Cap}_D}, \end{aligned}$$

where we used the fact that  $\mathcal{S}_D[\phi_0](\mathbf{x}) = -\text{Cap}_D^{-1}$  for all  $\mathbf{x} \in D$ .

- **Calculation of  $(\mathcal{A}_{3,0}[\Psi_0], \Phi_0)$ .** Similarly, using the second point of Lemma A.1, we get

$$(\mathcal{A}_{3,0}[\Psi_0], \Phi_0) = v_b^{-3} (\psi_0, \mathcal{K}_{D,3}[\mathbf{1}_{\partial D}]) = v_b^{-3} \left( \psi_0, \frac{i|D|}{4\pi} \mathbf{1}_{\partial D} \right) = \frac{i|D|}{4\pi v_b^3}.$$

- **Calculation of  $(\mathcal{A}_{0,1}[\Psi_0], \Phi_0)$ .** We directly have

$$(\mathcal{A}_{0,1}[\Psi_0], \Phi_0) = -(\psi_0, \mathbf{1}_{\partial D}) = -1.$$

- **Calculation of  $(\mathcal{A}_{0,1} \tilde{\mathcal{A}}_0^{-1} \mathcal{A}_{1,0}[\Psi_0], \Phi_0)$ .** We have

$$\begin{aligned} \mathcal{A}_{1,0}[\Psi_0] &= \begin{pmatrix} \frac{1}{v_b} - \frac{1}{v} \\ 0 \end{pmatrix} \begin{pmatrix} \mathcal{S}_{D,1}[\psi_0] \\ 0 \end{pmatrix} = \begin{pmatrix} \frac{1}{v_b} - \frac{1}{v} \\ 0 \end{pmatrix} \frac{-i}{4\pi} \begin{pmatrix} \mathbf{1}_{\partial D} \\ 0 \end{pmatrix}, \\ \mathcal{A}_{0,1}^*[\Phi_0] &= \begin{pmatrix} 0 \\ -(\frac{1}{2} + \mathcal{K}_D)[\mathbf{1}_{\partial D}] \end{pmatrix} = -\begin{pmatrix} 0 \\ \mathbf{1}_{\partial D} \end{pmatrix}. \end{aligned}$$

Let us calculate  $\tilde{\mathcal{A}}_0^{-1} \begin{pmatrix} \mathbf{1}_{\partial D} \\ 0 \end{pmatrix}$ . We look for  $(y_b, y) \in \mathcal{H}$  so that

$$\begin{pmatrix} \mathbf{1}_{\partial D} \\ 0 \end{pmatrix} = (\mathcal{A}_0 + \mathcal{P}_0) \begin{pmatrix} y_b \\ y \end{pmatrix} = \begin{pmatrix} \mathcal{S}_D[y_b - y] \\ (-\frac{1}{2} + \mathcal{K}_D^*)[y_b] \end{pmatrix} + (y_b + y, \psi_0) \begin{pmatrix} 0 \\ \mathbf{1}_{\partial D} \end{pmatrix}.$$

By solving the above equations directly, we obtain  $y_b = \frac{-\text{Cap}_D}{2}\psi_0$  and  $y = \frac{\text{Cap}_D}{2}\psi_0$ , so that

$$\tilde{\mathcal{A}}_0^{-1} \begin{pmatrix} \mathbf{1}_{\partial D} \\ 0 \end{pmatrix} = \frac{\text{Cap}_D}{2} \begin{pmatrix} -\psi_0 \\ \psi_0 \end{pmatrix}. \quad (2.10)$$

It follows that

$$\left( \mathcal{A}_{0,1} \tilde{\mathcal{A}}_0^{-1} \mathcal{A}_{1,0}[\Psi_0], \Phi_0 \right) = \left( \frac{1}{v_b} - \frac{1}{v} \right) \frac{i\text{Cap}_D}{8\pi}.$$

• **Calculation of**  $\left( \mathcal{A}_{2,0} \tilde{\mathcal{A}}_0^{-1} \mathcal{A}_{1,0}[\Psi_0], \Phi_0 \right)$ . Using similar calculations, we obtain

$$\begin{aligned} \left( \mathcal{A}_{2,0} \tilde{\mathcal{A}}_0^{-1} \mathcal{A}_{1,0}[\Psi_0], \Phi_0 \right) &= \left( \tilde{\mathcal{A}}_0^{-1} \mathcal{A}_{1,0}[\Psi_0], \mathcal{A}_{2,0}^*[\Phi_0] \right) \\ &= \frac{1}{v_b^2} \left( \frac{1}{v_b} - \frac{1}{v} \right) \frac{i\text{Cap}_D}{8\pi} (\psi_0, \mathcal{K}_{D,2}[\mathbf{1}_{\partial D}]) = \frac{1}{v_b^2} \left( \frac{1}{v_b} - \frac{1}{v} \right) \frac{i|D|}{8\pi}. \end{aligned}$$

• **Conclusion.** Considering the above the results, we can derive from (2.9) that

$$\begin{aligned} A(\omega, \delta) &= -\omega^2 \frac{|D|}{v_b^2 \text{Cap}_D} - \omega^3 \frac{i|D|}{8\pi v_b^2} \left( \frac{1}{v_b} + \frac{1}{v} \right) + \delta + \omega \delta \frac{i\text{Cap}_D}{8\pi} \left( \frac{1}{v_b} - \frac{1}{v} \right) \\ &\quad + O(|\omega|^4 + |\delta| |\omega|^2 + |\delta|^2). \end{aligned} \quad (2.11)$$

We now solve  $A(\omega, \delta) = 0$ . It is clear that  $\delta = O(\omega^2)$ , and thus  $\omega_0(\delta) = O(\sqrt{\delta})$ . We write  $\omega_0(\delta) = a_1 \delta^{\frac{1}{2}} + a_2 \delta + O(\delta^{\frac{3}{2}})$ , and get

$$\begin{aligned} & -\frac{|D|}{v_b^2 \text{Cap}_D} \left( a_1 \delta^{\frac{1}{2}} + a_2 \delta + O(\delta^{\frac{3}{2}}) \right)^2 - \frac{i|D|}{8\pi v_b^2} \left( \frac{1}{v_b} + \frac{1}{v} \right) \left( a_1 \delta^{\frac{1}{2}} + a_2 \delta + O(\delta^{\frac{3}{2}}) \right)^3 \\ & + \delta + \frac{i\text{Cap}_D}{8\pi} \left( \frac{1}{v_b} - \frac{1}{v} \right) \left( a_1 \delta^{\frac{3}{2}} + a_2 \delta^2 + O(\delta^{\frac{5}{2}}) \right) + O(\delta^2) = 0. \end{aligned}$$

From the coefficients of the  $\delta$  and  $\delta^{\frac{3}{2}}$  terms, we obtain

$$-a_1^2 \frac{|D|}{v_b^2 \text{Cap}_D} + 1 = 0 \quad \text{and} \quad 2a_1 a_2 \frac{-|D|}{v_b^2 \text{Cap}_D} - a_1^3 \frac{i|D|}{8\pi v_b^2} \left( \frac{1}{v_b} + \frac{1}{v} \right) + a_1 \frac{i\text{Cap}_D}{8\pi} \left( \frac{1}{v_b} - \frac{1}{v} \right) = 0$$

which yields

$$a_1 = \pm \sqrt{\frac{v_b^2 \text{Cap}_D}{|D|}} \quad \text{and} \quad a_2 = -\frac{i\text{Cap}_D^2 v_b^2}{8\pi |D| v}.$$

This completes the proof of the theorem. □

**Remark 2.4.** Using the method developed above, we can also obtain the full asymptotic expansion for the resonance with respect to the small parameter  $\delta$ .

### 3 The point scatterer approximation

In this section, we derive the *monopole approximation*. In order to do so, we change the point of view. We now assume that the size of the bubble goes to 0, and we would like to replace the complicated behavior of the bubble by an equivalent simple formula (monopole approximation). More specifically, we assume that  $\mathbf{0} \in D$  and that the bubble is  $D_\varepsilon := \varepsilon D$ , with contrast  $\delta_\varepsilon$ , for some  $\varepsilon > 0$ . We excite the bubble at a fixed frequency  $u_{\mathbf{k}}^{\text{in}} := u_0 e^{i\mathbf{k} \cdot \mathbf{x}}$ , and we would like to understand the behavior of the scattered field as  $\varepsilon \rightarrow 0$ . As noted in the previous section, the interesting regime is when  $\sqrt{\delta_\varepsilon} \sim \varepsilon$ . In the sequel, we fix  $\mu \geq 0$ , and study the limit as  $\varepsilon \rightarrow 0$  of  $u^s(\mathbf{x})$  solution to (2.1) for a bubble  $\varepsilon|D|$  with contrast  $\delta_\varepsilon := \mu\varepsilon^2$ .

**Theorem 3.1.** *For all  $\mathbf{x} \in \mathbb{R}^3 \setminus \{\mathbf{0}\}$  and in the regime where the bubble  $D_\varepsilon$  with contrast  $\delta = \mu\varepsilon^2$  is excited by  $u_{\mathbf{k}}^{\text{in}} := u_0 e^{i\mathbf{k} \cdot \mathbf{x}}$ , it holds that*

$$u^s(\mathbf{x}) = \begin{cases} \varepsilon \left( \frac{\text{Cap}_D}{1 - \frac{\mu_M}{\mu}} u_0 \right) G_k(\mathbf{x}) + O(\varepsilon^2) & \text{if } \mu \neq \mu_M \\ i \frac{4\pi}{k} u_0 G_k(\mathbf{x}) + O(\varepsilon) & \text{if } \mu = \mu_M, \end{cases}$$

where we set

$$\mu_M := \frac{|D|\omega^2}{\text{Cap}_D v_b^2} = \frac{|D|k_b^2}{\text{Cap}_D}. \quad (3.1)$$

**Remark 3.1.** *Loosely speaking, if the bubble is small and has a high-contrast, then according to Theorem 3.1, the scattered field behaves like*

$$u^s \approx \frac{\text{Cap}_D}{\left(1 - \frac{|D|\omega^2}{\text{Cap}_D v_b^2 \delta}\right) - i \frac{\text{Cap}_D k}{4\pi}} u_{\mathbf{k}}^{\text{in}}(\mathbf{0}) G_k \approx g_s(\omega) u_{\mathbf{k}}^{\text{in}}(\mathbf{0}) G_{k_0},$$

where the function  $g_s(\omega)$ , called the scattering function of the bubble, is defined by

$$g_s(\omega) := \frac{\text{Cap}_D}{\left(1 - \frac{\omega^2}{\omega_M^2}\right) - i \frac{\text{Cap}_D k}{4\pi}}.$$

Here,  $\omega_M := \sqrt{\frac{\text{Cap}_D \delta}{|D|}} v_b$  is the Minnaert resonance of the bubble.

**Remark 3.2.** *The imaginary part in the denominator of  $g_s$  is called the radiative damping term. Since this term is negative, the poles of  $\omega \rightarrow g_s(\omega)$  have a negative imaginary part. Together with the Titchmarsh's theory [22], this implies that  $g_s$  is the Fourier transform of a causal function, hence satisfies the Kramers-Krönig relations.*

**Remark 3.3.** *If the bubble is a sphere of radius  $R$ , one obtains*

$$g_s(\omega) = \frac{4\pi R}{\left(1 - \frac{\omega^2}{\omega_M^2}\right) - i R k}.$$

*This term has the same properties as the usual scattering functions that we may find in [10, 17].*



*Proof of Theorem 3.1.* By a simple change of scale, the problem is equivalent to understanding the behavior of  $\mathcal{S}_D^{\varepsilon k}[\psi](\mathbf{x}/\varepsilon)$  as  $\varepsilon \rightarrow 0$ , where  $\Psi = (\psi_b, \psi)$  is solution to

$$\mathcal{A}(\varepsilon\omega, \mu\varepsilon^2)\Psi = F \quad \text{with} \quad F(\mathbf{x}) := u_0 \begin{pmatrix} e^{i\varepsilon\mathbf{k}\cdot\mathbf{x}} \\ \mu\varepsilon^3 i\mathbf{k} \cdot \nu_{\mathbf{x}} e^{i\mathbf{k}\cdot\mathbf{x}} \end{pmatrix}.$$

**Step 1.** We write  $\Psi = \alpha\Psi_0 + \Psi_1$  with  $(\Psi_1, \Psi_0) = 0$ . Then,

$$(\tilde{\mathcal{A}}_0 - \mathcal{P}_0 + \mathcal{B})[\alpha\Psi_0 + \Psi_1] = F$$

implies that

$$\left(1 - (\tilde{\mathcal{A}}_0 + \mathcal{B})^{-1}\mathcal{P}_0\right)[\alpha\Psi_0 + \Psi_1] = (\tilde{\mathcal{A}}_0 + \mathcal{B})^{-1}[F],$$

which yields

$$\alpha\Psi_0 + \Psi_1 - \alpha\|\Psi_0\|^2(\tilde{\mathcal{A}}_0 + \mathcal{B})^{-1}[\Phi_0] = (\tilde{\mathcal{A}}_0 + \mathcal{B})^{-1}[F].$$

As a result, we get

$$\begin{cases} \alpha = \frac{((\tilde{\mathcal{A}}_0 + \mathcal{B})^{-1}[F], \Psi_0)}{\|\Psi_0\|^2 \left(1 - ((\tilde{\mathcal{A}}_0 + \mathcal{B})^{-1}[\Phi_0], \Psi_0)\right)} = -\frac{((\tilde{\mathcal{A}}_0 + \mathcal{B})^{-1}[F], \Psi_0)}{\tilde{A}(\omega, \delta)}, \\ \Psi_1 = (\tilde{\mathcal{A}}_0 + \mathcal{B})^{-1}[F] + \alpha\|\Psi_0\|^2(\tilde{\mathcal{A}}_0 + \mathcal{B})^{-1}[\Phi_0] - \alpha\Psi_0. \end{cases}$$

We have  $F = u_0 \begin{pmatrix} \mathbb{1}_{\partial D} \\ 0 \end{pmatrix} + O(\varepsilon)$ , so that, together with (2.10),

$$(\tilde{\mathcal{A}}_0 + \mathcal{B})^{-1}[F] = u_0(\tilde{\mathcal{A}}_0 + \mathcal{B})^{-1} \begin{pmatrix} \mathbb{1}_{\partial D} \\ 0 \end{pmatrix} + O(\varepsilon) = u_0 \tilde{\mathcal{A}}_0^{-1} \begin{pmatrix} \mathbb{1}_{\partial D} \\ 0 \end{pmatrix} + O(\varepsilon) = u_0 \frac{\text{Cap}_D}{2} \begin{pmatrix} -\psi_0 \\ \psi_0 \end{pmatrix} + O(\varepsilon).$$

As a result,

$$\Psi_1 = u_0 \frac{\text{Cap}_D}{2} \begin{pmatrix} -\psi_0 \\ \psi_0 \end{pmatrix} + O(\varepsilon).$$

**Step 2.** To calculate the scattered field, we use the approximation

$$\begin{aligned} \mathcal{S}_D^{\varepsilon k}[\psi_0](\mathbf{x}/\varepsilon) &= \int_{\partial D} G_{\varepsilon k} \left( \left| \frac{\mathbf{x}}{\varepsilon} - \mathbf{y} \right| \right) \psi_0(\mathbf{y}) d\sigma(\mathbf{y}) = -\varepsilon \int_{\partial D} \frac{e^{ik|\mathbf{x}-\varepsilon\mathbf{y}|}}{4\pi|\mathbf{x}-\varepsilon\mathbf{y}|} \psi_0(\mathbf{y}) d\sigma(\mathbf{y}) \\ &= -\varepsilon \frac{e^{ik|\mathbf{x}|}}{4\pi|\mathbf{x}|} \int_{\partial D} \psi_0(\mathbf{y}) d\sigma(\mathbf{y}) + O(\varepsilon^2) = -\varepsilon \frac{e^{ik|\mathbf{x}|}}{4\pi|\mathbf{x}|} + O(\varepsilon^2) = \varepsilon G_k(\mathbf{x}) + O(\varepsilon^2). \end{aligned}$$

Therefore,

$$u^s(\mathbf{x}/\varepsilon) = \left( \alpha + u_0 \frac{\text{Cap}}{2} + O(\varepsilon) \right) \mathcal{S}_D^{\varepsilon k}[\psi_0](|\mathbf{x}_0|/\varepsilon) = \varepsilon \left( \alpha + u_0 \frac{\text{Cap}}{2} \right) G_k(\mathbf{x})(1 + O(\varepsilon)).$$

**Step 3.** We now calculate the coefficient  $\alpha$ . We write

$$F = F_1 + F_2 \quad \text{with} \quad F_1 = u_0 \begin{pmatrix} e^{i\mathbf{k} \cdot \mathbf{x}} \\ 0 \end{pmatrix} \quad \text{and} \quad F_2 = \begin{pmatrix} 0 \\ \mu \varepsilon^3 i k e^{i\mathbf{k} \cdot \mathbf{x}} \end{pmatrix}.$$

It is clear that  $F_2 = O(\varepsilon^3)$ , so that

$$\begin{aligned} \alpha &= -\frac{((\tilde{\mathcal{A}}_0 + \mathcal{B})^{-1}[F], \Psi_0)}{\tilde{A}(\omega, \delta)} = -\frac{((\tilde{\mathcal{A}}_0 + \mathcal{B})^{-1}[F_1], \Psi_0) + O(\varepsilon^3)}{\tilde{A}(\omega, \delta)} \\ &= -\frac{\|\Phi_0\|^2 ((\tilde{\mathcal{A}}_0 + \mathcal{B})^{-1}[F_1], \Psi_0) + O(\varepsilon^3)}{A(\omega, \delta)}. \end{aligned}$$

We have, from the Neumann series,

$$\begin{aligned} ((\tilde{\mathcal{A}}_0 + \mathcal{B})^{-1}[F_1], \Psi_0) &= ((\tilde{\mathcal{A}}_0^{-1} - \tilde{\mathcal{A}}_0^{-1} \mathcal{B} \tilde{\mathcal{A}}_0^{-1} + \tilde{\mathcal{A}}_0^{-1} \mathcal{B} \tilde{\mathcal{A}}_0^{-1} \mathcal{B} \tilde{\mathcal{A}}_0^{-1})[F_1], \Psi_0) + O(\varepsilon^3) \\ &= \|\Phi_0\|^{-2} \left( (F_1, \Phi_0) - (\tilde{\mathcal{A}}_0^{-1}[F_1], \mathcal{B}^* \Phi_0) + (\tilde{\mathcal{A}}_0^{-1} \mathcal{B} \tilde{\mathcal{A}}_0^{-1}[F_1], \mathcal{B}^*[\Phi_0]) \right) + O(\varepsilon^3) \\ &= \|\Phi_0\|^{-2} \left( -(\tilde{\mathcal{A}}_0^{-1}[F_1], \mathcal{B}^*[\Phi_0]) + (\tilde{\mathcal{A}}_0^{-1} \mathcal{B} \tilde{\mathcal{A}}_0^{-1}[F_1], \mathcal{B}^*[\Phi_0]) \right) + O(\varepsilon^3), \end{aligned}$$

where we have used the fact that  $(\tilde{\mathcal{A}}_0^*)^{-1}[\Psi_0] = \|\Phi_0\|^{-2} \Phi_0$  and that  $(F_1, \Phi_0) = 0$ . Recall that

$$\mathcal{B}^*[\Phi_0] = \varepsilon \omega \mathcal{A}_{1,0}^*[\Phi_0] + \varepsilon^2 \omega^2 \mathcal{A}_{2,0}^*[\Phi_0] + \varepsilon^2 \mu \mathcal{A}_{0,1}^*[\Phi_0] + O(\varepsilon^3).$$

Together with

$$\tilde{\mathcal{A}}_0^{-1}[F_1] = u_0 \frac{\text{Cap}_D}{2} \begin{pmatrix} -\psi_0 \\ \psi_0 \end{pmatrix} + O(\varepsilon),$$

and

$$\mathcal{A}_{1,0}^*[\Phi_0] = 0, \quad \mathcal{A}_{2,0}^*[\Phi_0] = \begin{pmatrix} v_b^{-2} \mathcal{K}_{D,2}[\mathbb{1}_{\partial D}] \\ 0 \end{pmatrix}, \quad \mathcal{A}_{0,1}^*[\Phi_0] = -\begin{pmatrix} 0 \\ \mathbb{1}_{\partial D} \end{pmatrix},$$

we can conclude that

$$\begin{aligned} \|\Phi_0\|^2 ((\tilde{\mathcal{A}}_0 + \mathcal{B})^{-1}[F_1], \Psi_0) &= \varepsilon^2 u_0 \frac{\text{Cap}_D}{2} [-\omega^2(\psi_0, v_b^{-2} \mathcal{K}_{D,2}[\mathbb{1}_{\partial D}]) - \mu(\psi_0, \mathbb{1}_{\partial D})] + O(\varepsilon^3) \\ &= -\varepsilon^2 u_0 \frac{\text{Cap}_D}{2} (\mu_M + \mu) + O(\varepsilon^3), \end{aligned}$$

where  $\mu_M$  was defined in (3.1).

On the other hand, from the expression of  $A(\omega, \delta)$  in (2.11), we have

$$A(\omega, \delta) = \varepsilon^2 (\mu - \mu_M) + \varepsilon^3 \left( \omega \mu \frac{i \text{Cap}_D}{8\pi} \left( \frac{1}{v_b} - \frac{1}{v} \right) - \omega^3 \frac{i|D|}{8\pi v_b^2} \left( \frac{1}{v_b} + \frac{1}{v} \right) \right) + O(\varepsilon^4). \quad (3.2)$$

If  $\mu \neq \mu_M$ , the first term is dominant, and we get

$$\alpha = u_0 \frac{\text{Cap}(\mu + \mu_M)}{2(\mu - \mu_M)} + O(\varepsilon) \quad \text{so that} \quad \alpha + u_0 \frac{\text{Cap}}{2} = u_0 \frac{\text{Cap}_D}{1 - \frac{\mu_M}{\mu}} + O(\varepsilon).$$

If  $\mu = \mu_M$ , then the second term in (3.2) is dominant. Actually, this term simplifies into

$$\omega \mu_M \frac{i \text{Cap}_D}{8\pi} \left( \frac{1}{v_b} - \frac{1}{v} \right) - \omega^3 \frac{i|D|}{8\pi v_b^2} \left( \frac{1}{v_b} + \frac{1}{v} \right) = i \frac{\omega^3 |D|}{4\pi v_b^2 v} = -i \mu_M \frac{\omega \text{Cap}_D}{4\pi v},$$

so that

$$\alpha = i \frac{u_0}{\varepsilon} \frac{4\pi v}{\omega} + O(1) \quad \text{so that} \quad \alpha + u_0 \frac{\text{Cap}}{2} = \alpha + O(1) = i \frac{u_0}{\varepsilon} \frac{4\pi v}{\omega} + O(1).$$

This concludes the proof of Theorem 3.1.  $\square$

**Remark 3.4.** *Using similar methods together with the results of Appendix B, we can derive the monopole approximation in two dimensions.*

## 4 Numerical illustrations

In this section we perform numerical simulations in two dimensions to analyze the resonant frequencies for two scenarios. We first analyze the single bubble case for which a formula was derived in Theorem B.1. We then calculate the resonant frequencies for two bubbles and compare our results with the single bubble case.

### 4.1 Resonant frequency of a single bubble in two dimensions

To validate the Minnaert resonance formula (B.3) in two dimensions we first determine the characteristic value  $\omega_c$  of  $\mathcal{A}(\omega, \delta)$  in (2.4) numerically. We then calculate the complex root  $\omega_f$  of (B.3) that has a positive real part. Comparing  $\omega_c$  and  $\omega_r$  over a range of appropriate values of  $\delta$  allows us to judge the accuracy of the formula.

In order to perform the analysis in the correct regime, which was described in Section 2, we take  $\rho = \kappa = 1000$  and  $\rho_b = \kappa_b = c$ , where  $c$  is chosen such that the wave speed in both air and water is of order 1 and  $\delta \in \{10^{-i}\}$ ,  $i \in \{1, \dots, 5\}$ . We use  $2^9$  points to discretize the unit circle used in the calculation of the layer potentials that form  $\mathcal{A}$ . Calculating  $\omega_c$  is equivalent to determining the smallest  $\omega$  such that  $\mathcal{A}(\omega, \delta)$  has a zero eigenvalue, *i.e.*

$$\omega_c := \arg \min_{\omega \in \mathbb{C}} \{|\omega|, 0 \in \sigma(\mathcal{A}(\omega, \delta))\}.$$

We denote by  $\lambda(\omega)$  the eigenvalue of  $\mathcal{A}(\omega, \delta)$  with the smallest norm. We find the complex roots of the equation  $\lambda(\omega) = 0$  using Muller's method [2, 9]. We also use Muller's method to calculate  $\omega_f$  solution to (B.3). The resonant frequencies  $\omega_c$  and  $\omega_f$ , along with the relative errors, for specific values of  $\delta$  are given in Table 1. In Figure 1 it can be seen that the relative error becomes very small when  $\delta \ll 1$ , confirming the excellent accuracy of the formula. In particular, we note that when  $\delta = 10^{-3}$ , which is close to the usual contrast between water and air, the difference between  $\omega_c$  and  $\omega_f$  is negligible with a relative error of only 0.0652%.

### 4.2 Resonant frequencies of two bubbles in two dimensions

In this subsection we numerically solve the two bubble case and analyze it with respect to our results for the Minnaert resonance of a single bubble. In the case of two bubbles we have two

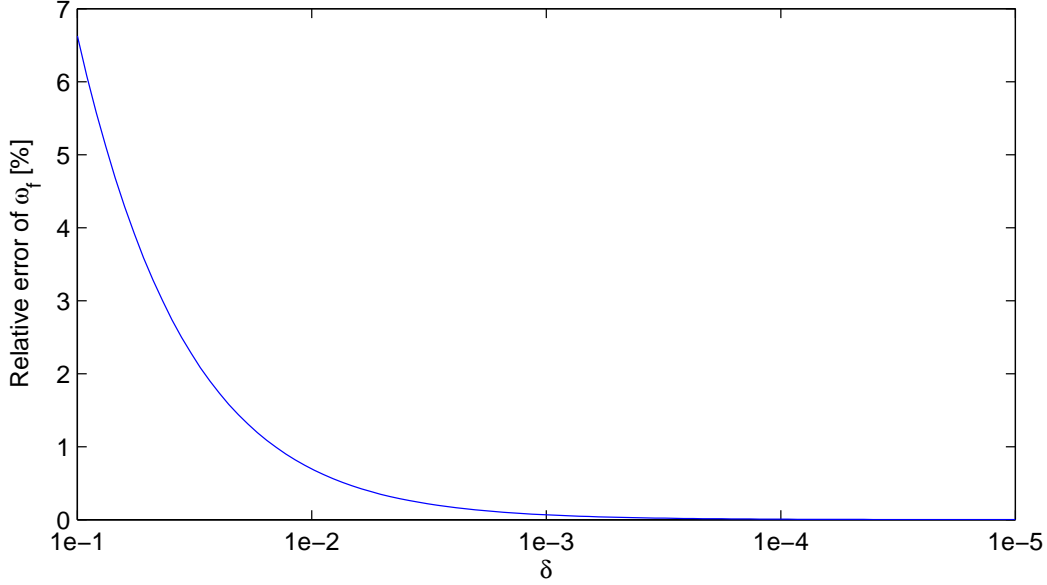


Figure 1: The relative error of the Minnaert resonance  $\omega_c$  obtained by the two dimensional formula (B.3) becomes negligible when we are in the appropriate high contrast regime.

$\delta$	$\omega_c$	$\omega_f$	Relative error
$10^{-1}$	$0.261145 - 0.150949i$	$0.250455 - 0.134061i$	5.8203%
$10^{-2}$	$0.075146 - 0.023976i$	$0.074681 - 0.023687i$	0.6727%
$10^{-3}$	$0.021001 - 0.004513i$	$0.020987 - 0.004508i$	0.0652%
$10^{-4}$	$0.005950 - 0.000959i$	$0.005949 - 0.000959i$	0.0062%
$10^{-5}$	$0.001714 - 0.000221i$	$0.001714 - 0.000221i$	0.0030%

Table 1: A comparison between the characteristic value  $\omega_c$  of  $\mathcal{A}(\omega, \delta)$  and the root of the two dimensional resonance formula (B.3) with positive real part  $\omega_f$ , over several values of  $\delta$ .

resonant frequencies,  $\omega_s$  and  $\omega_a$ , that correspond to the normal modes of the system [11]. These frequencies are not in general equal to the one bubble resonant frequency  $\omega_c$ . The interaction between the bubbles gives rise to a shift in the resonance frequencies. The symmetric mode  $\omega_s$  typically shows a downward frequency shift and occurs when the bubbles oscillate (collapse and expand) in phase, essentially opposing each other's motion. The antisymmetric mode  $\omega_a$  shows an upward frequency shift and occurs when the bubbles oscillate in antiphase, facilitating each other's motion.

To account for the interaction between the two bubbles the matrix  $\mathcal{A}$  in (2.3) is replaced with

$$\mathcal{A}_2(\omega, \delta) = \begin{pmatrix} \mathcal{S}_{D_1}^{k_b} & -\mathcal{S}_{D_1}^k & 0 & -\mathcal{S}_{D_1, D_2}^k \\ -\frac{1}{2} + \mathcal{K}_{D_1}^{k_b, *} & -\delta(\frac{1}{2} + \mathcal{K}_{D_1}^{k, *}) & 0 & -\mathcal{K}_{D_1, D_2}^{k, *} \\ 0 & -\mathcal{S}_{D_2, D_1}^k & \mathcal{S}_{D_2}^{k_b} & -\mathcal{S}_{D_2}^k \\ 0 & -\mathcal{K}_{D_2, D_1}^{k, *} & -\frac{1}{2} + \mathcal{K}_{D_2}^{k_b, *} & -\delta(\frac{1}{2} + \mathcal{K}_{D_2}^{k, *}) \end{pmatrix},$$

where the operators  $\mathcal{S}_{D_i, D_j}^k$  and  $\mathcal{K}_{D_i, D_j}^{k,*}$  are given, for  $\mathbf{x} \in \partial D_i$  by

$$\mathcal{S}_{D_i, D_j}^k = \int_{\partial D_j} G_k(\mathbf{x}, \mathbf{y}) \psi(\mathbf{y}) d\sigma(\mathbf{y}) \quad \text{and} \quad \mathcal{K}_{D_i, D_j}^{k,*}[\psi](\mathbf{x}) = \int_{\partial D_j} \frac{\partial G_k(\mathbf{x}, \mathbf{y})}{\partial \nu_{\mathbf{x}}} \psi(\mathbf{y}) d\sigma(\mathbf{y}).$$

The variation in the eigenvalues of  $\mathcal{A}_2$  with respect to the input frequency, and hence the shifting of the resonant frequencies, is highly sensitive to the ratio of  $\delta = \rho_b/\rho$  to  $\kappa_b/\kappa$ , with it being at a minimum when these quantities are equal. In order to make the results more clearly visible, while keeping the simulation in the correct regime, let us take  $\rho_b = 1.1$  and  $\kappa_b = 0.1$ . For reference, we note that the resonant frequency for a single bubble in this regime is  $\omega_c = 0.01856427 - 0.00387243i$ .

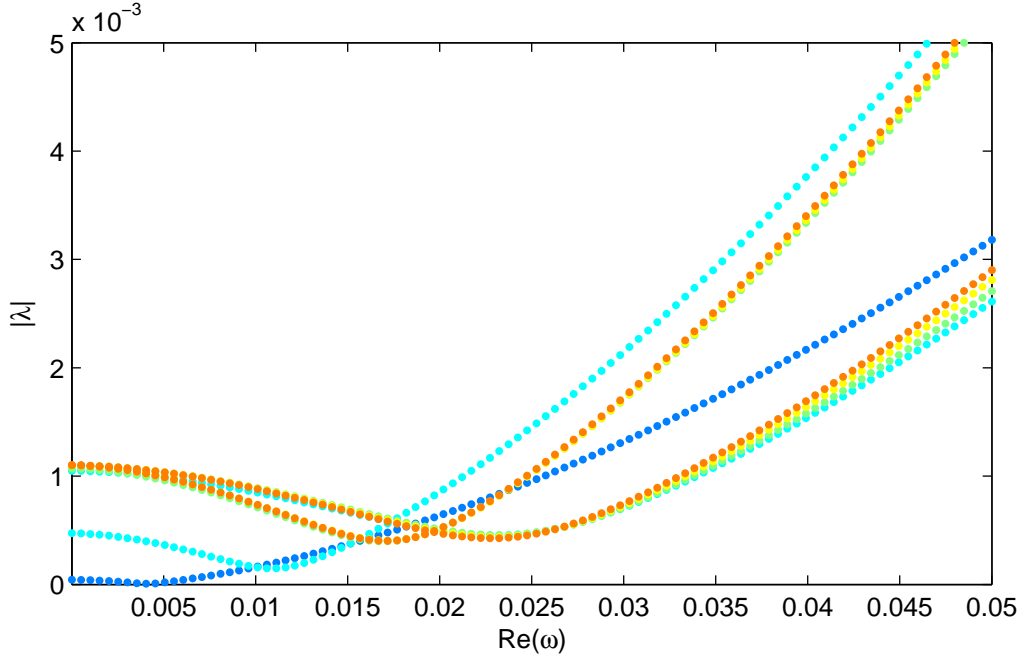


Figure 2: When the bubbles are close together the resonance may be much more pronounced. Here we have  $|\lambda|$  as the distance varies from  $d = 0.1$  (blue dots) to  $d = 0.5$  (orange dots) and  $\Im(\omega) = -0.0008i$ . We have resonance at the symmetric mode  $\omega_s \approx 0.0041 - 0.0008i$  when  $d = 0.1$ . The resonant frequency of a single bubble is  $\omega_c = 0.01856427 - 0.00387243i$ .

We now identify three regimes in terms of bubble separation distance  $d$ . The first occurs due to strong interaction when  $d$  is less than the radius of the bubbles. In this regime the resonant frequency shift may be much more pronounced. For example, when  $d = 0.1$  we have  $\omega_s \approx 0.0041 - 0.0008i$ , while  $\omega_a \approx 0.7435 + 0.0032i$ . This regime is shown in Figure 2 for  $\Im(\omega) = -0.008i$ .

When  $d$  is greater than the radius of the bubbles, yet not very large, we have a somewhat stable regime featuring small to moderate resonant frequency shifts. It is natural to expect that as the distance between the bubbles increases, the eigenvalues of the two bubble system approach those of the single bubble system. And indeed that is the case as can be seen in Figure 3 where  $\omega$  has been restricted to  $\mathbb{R}$ .

	$d = 10$	$d = 100$
$\omega_s$	$0.01722793 - 0.00407516 i$	$0.01819212 - 0.00316674 i$
$\omega_a$	$0.02025476 - 0.00349214 i$	$0.01905723 - 0.00470526 i$

Table 2: The normal modes of the two bubble system shown in Figure 4. They are quite close to the resonant frequency of a single bubble in this regime, in contrast to the strong frequency shifts observed when  $d \ll a$  and  $d \gg a$ .

As with the three dimensional case, however, we require a complex  $\omega$  with negative imaginary part in order for  $\mathcal{A}$  or  $\mathcal{A}_2$  to become singular. This can be seen in Figure 4 for  $d = 10$  and  $d = 100$ . Table 2 shows that the normal modes are quite close to the single bubble resonant frequency in this regime.

The final regime occurs when the separation distance becomes very large compared to the radius of the bubbles. In this situation the sensitivity of the Hankel function in the layer potentials to negative imaginary numbers becomes apparent, leading to a much wider variation in the eigenvalues of  $\mathcal{A}_2$ . Similarly to when the bubbles are very close together, we observe significant resonant frequency shifts in this regime. When  $d$  varies from 100 to 1000 we obtain the spectrum shown in Figure 5. Here we have a symmetric mode  $\omega_s \approx 0.0013 - 0.00577 i$  and an antisymmetric mode  $\omega_a \approx 0.0308 - 0.00575 i$ .

## 5 Concluding remarks

In this paper we have investigated the acoustic wave propagation problem in bubbly media and for the first time rigorously derived the low frequency resonances. Furthermore, we have provided a justification for the monopole approximation. The techniques developed in this paper open a door for a mathematical and numerical framework for investigating acoustic wave propagation in bubbly media. In forthcoming papers we will investigate the superabsorption effect that can be achieved using bubble metascreens [18, 20]. We will also mathematically justify Foldy's approximation and quantify time-reversal and the superfocusing effect in bubbly media probed at their Minnaert resonant frequency [17]. Finally, we will develop accurate and fast numerical schemes for solving acoustic wave propagation problems in the presence of closely spaced bubbles.

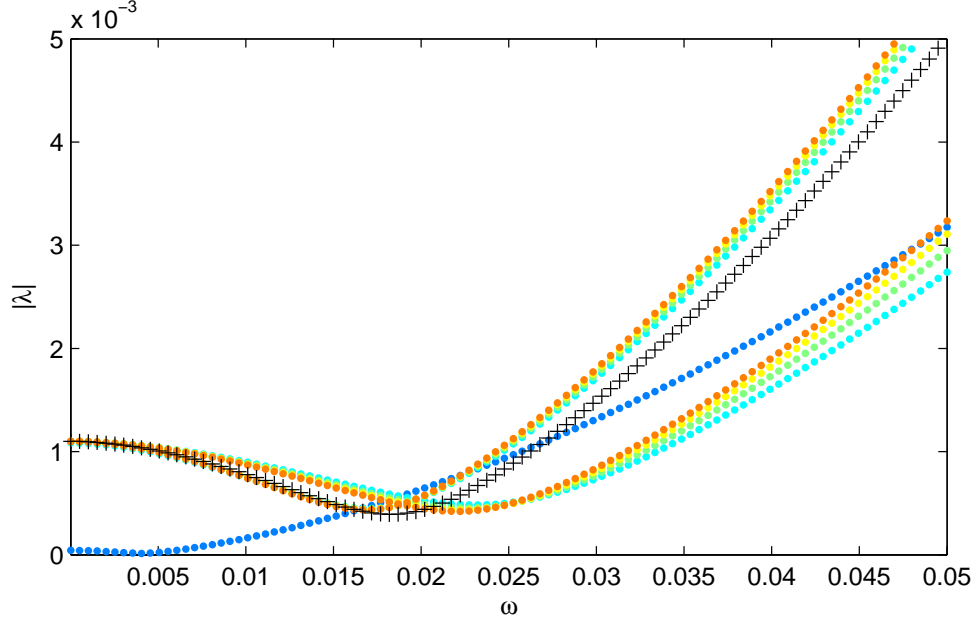
## A Some asymptotic expansions

We recall some basic asymptotic expansion for the layer potentials in three and two dimensions from [2] (see also the appendix in [3]).

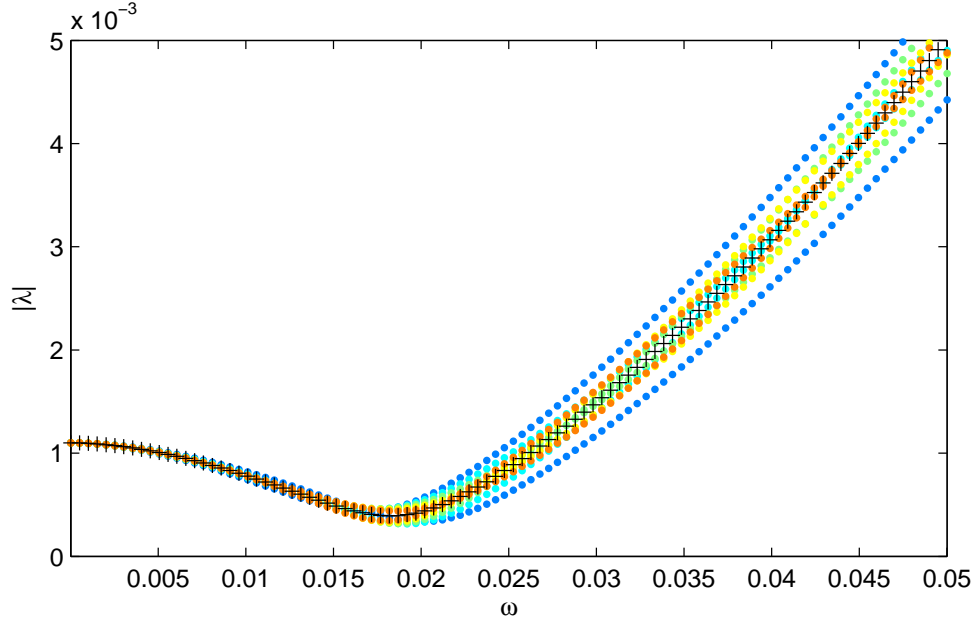
### A.1 Some asymptotic expansions in three dimensions

We expand the Green's function  $G_k$  with

$$G_k(\mathbf{x}) = -\frac{e^{ik|\mathbf{x}|}}{4\pi|\mathbf{x}|} = G_0(\mathbf{x}) + \sum_{n=1}^{\infty} k^n G_n(\mathbf{x}), \quad \text{with} \quad G_n(\mathbf{x}) := -\frac{i^n}{4\pi n!} |\mathbf{x}|^{n-1}. \quad (\text{A.1})$$

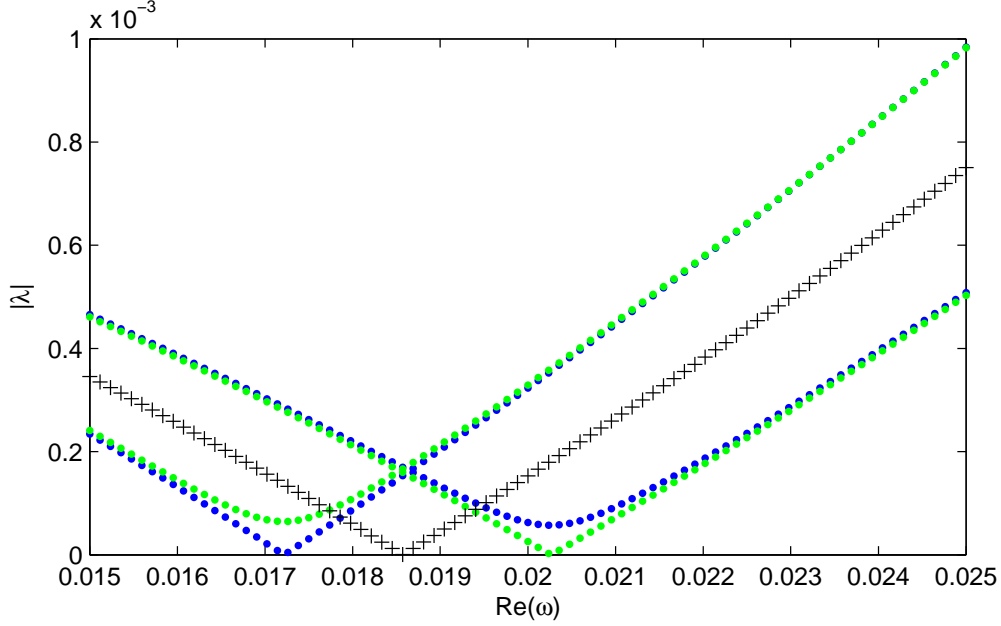


(a) The distance between the bubbles is varying from 0.1 to 1.

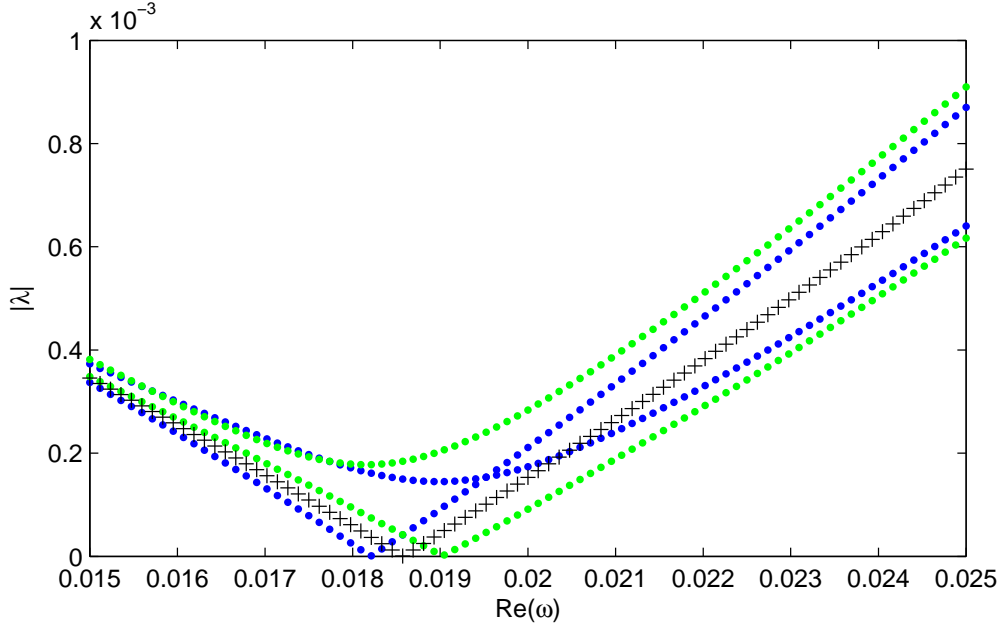


(b) The distance between the bubbles is varying from 10 to 100.

Figure 3:  $|\lambda|$  when  $\omega \in \mathbb{R}$  for  $\lambda \in \sigma(\mathcal{A})$  (black crosses) and  $\lambda \in \sigma(\mathcal{A}_2)$  (colored dots). The distance increases as the dots change from blue to orange. Although the eigenvalues of  $\mathcal{A}_2$  approach those of  $\mathcal{A}$  as the distance increases, they don't go to zero when  $\omega$  is real. Here,  $\sigma(\mathcal{A})$  and  $\mathcal{A}_2$  are the spectra of  $\mathcal{A}$  and  $\sigma(\mathcal{A}_2)$ , respectively.



(a) The distance between the bubbles is 10.



(b) The distance between the bubbles is 100.

Figure 4: The eigenvalues of  $\mathcal{A}$  (black crosses) and  $\mathcal{A}_2$  (blue and green dots) may go to zero in the regime where the bubbles are a moderate distance apart, provided  $\omega$  has some negative imaginary part. The frequency shift is less pronounced when  $d = 100$  as opposed to  $d = 10$  due to the decrease in the interaction of the bubbles with each other.



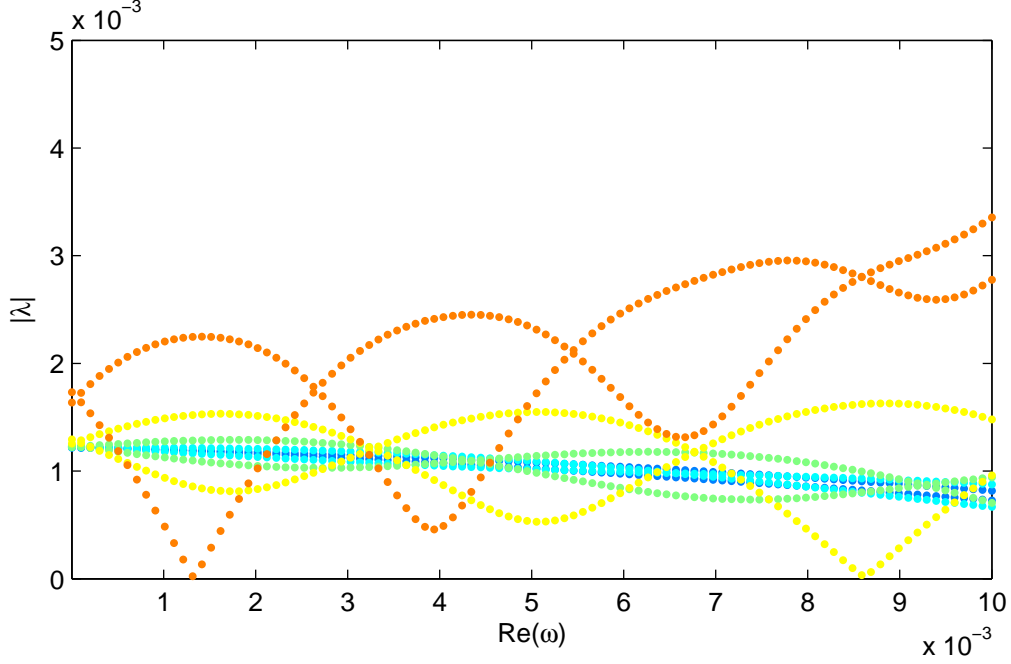


Figure 5: The sensitivity of the Hankel function in the layer potentials to negative imaginary numbers is apparent when the distance between the bubbles is very large. This leads to a signification reduction in the real part of the resonant frequencies. Here  $d$  varies from 100 to 1000 and  $\Im(\omega) = -0.00577i$ . We have a symmetric mode at  $\omega_s \approx 0.0013 - 0.00577i$ .

In particular,  $G_1(\mathbf{x}) = -\frac{i}{4\pi}$ . Developping in power of  $k$  the equation  $(\Delta + k^2)G_k = \delta_0$  leads to

$$\forall n \geq 1, \quad \Delta G_{n+2} = -G_n. \quad (\text{A.2})$$

From (A.1), we decompose the single layer potential as

$$\mathcal{S}_D^k = \mathcal{S}_D + \sum_{n=1}^{\infty} k^n \mathcal{S}_{D,n} \quad \text{with} \quad \mathcal{S}_{D,n}[\psi] := \int_{\partial D} G_n(\mathbf{x} - \mathbf{y}) \psi(\mathbf{y}) d\mathbf{y}, \quad (\text{A.3})$$

where the convergence holds in  $\mathcal{B}(L^2(\partial D), H^1(\partial D))$ . Similarly, the asymptotic expansion for the operator  $\mathcal{K}_D^{k,*}$  is

$$\mathcal{K}_D^{k,*}[\psi](x) = \mathcal{K}_D^* + \sum_{n=1}^{\infty} k^n \mathcal{K}_{D,n}^* \quad \text{with} \quad \mathcal{K}_{D,n}^*[\psi] := \int_{\partial D} \frac{\partial G_n(\mathbf{x} - \mathbf{y})}{\partial \nu_{\mathbf{x}}} \psi(\mathbf{y}) d\mathbf{y}, \quad (\text{A.4})$$

where the convergence holds in  $\mathcal{B}(L^2(\partial D), L^2(\partial D))$ . Using (A.2), we deduce the following useful identities.

**Lemma A.1.** *It holds:*

$$(i) \quad \mathcal{K}_{D,2}[\mathbb{1}_{\partial D}](x) = \int_{\partial D} \frac{\partial G_2(\mathbf{x} - \mathbf{y})}{\partial \nu_{\mathbf{y}}} d\sigma(\mathbf{y}) = \int_D \Delta_{\mathbf{y}} G_2(\mathbf{x} - \mathbf{y}) d\mathbf{y} = - \int_D G_0(\mathbf{x} - \mathbf{y}) d\mathbf{y},$$

$$(ii) \quad \mathcal{K}_{D,3}[\mathbb{1}_{\partial D}](x) = \int_{\partial D} \frac{\partial G_3(\mathbf{x} - \mathbf{y})}{\partial \nu_{\mathbf{y}}} d\sigma(\mathbf{y}) = \int_D \Delta_{\mathbf{y}} G_3(\mathbf{x} - \mathbf{y}) d\mathbf{y} = - \int_D G_1(\mathbf{x} - \mathbf{y}) d\mathbf{y} = \frac{i|D|}{4\pi}.$$

## A.2 Some asymptotic expansions in two dimensions

In two dimensions, the Green's function for the Laplace and Helmholtz equations are respectively

$$G_0 := \frac{1}{2\pi} \ln(|\mathbf{x}|) \quad \text{and} \quad \forall k > 0, \quad G_k(\mathbf{x}) := -\frac{i}{4} H_0^{(1)}(k|\mathbf{x}|)$$

and  $H_0^{(1)}$  is the Hankel function of first kind and order 0. We have

$$G_k(\mathbf{x}) = G_0(\mathbf{x}) + \eta_k + \sum_{n=1}^{\infty} (k^{2n} \ln k) G_n^{(1)}(\mathbf{x}) + k^{2n} G_n^{(2)}(\mathbf{x})$$

where we defined

$$G_n^{(1)}(\mathbf{x}) := b_n |\mathbf{x}|^{2n} \quad \text{and} \quad G_n^{(2)}(\mathbf{x}) := (b_n \ln |\mathbf{x}| + c_n) (|\mathbf{x}|)^{2n},$$

with

$$\eta_k := \frac{\ln k}{2\pi} + \eta_1, \quad \eta_1 := \frac{1}{2\pi} \left( \gamma - \ln 2 - \frac{i\pi}{2} \right), \quad b_n = \frac{(-1)^n}{2\pi 2^{2n} (n!)^2}, \quad c_n = b_n \left( 2\pi \eta_1 - \sum_{j=1}^n \frac{1}{j} \right),$$

and where  $\gamma$  is the Euler constant. The single-layer potential for the Helmholtz equation is defined by

$$\mathcal{S}_D^k[\psi] = \int_{\partial D} G_k(\cdot - \mathbf{y}) \psi(\mathbf{y}) d\sigma(\mathbf{y}) = \hat{\mathcal{S}}_D^k[\psi] + \sum_{n=1}^{\infty} (k^{2n} \ln k) \mathcal{S}_{D,n}^{(1)}[\psi] + k^{2n} \mathcal{S}_{D,n}^{(2)}[\psi],$$

where the convergence holds in  $\mathcal{B}(L^2(\partial D), H^1(\partial D))$ , and where we set

$$\hat{\mathcal{S}}_D^k[\psi] = \mathcal{S}_D[\psi] + \eta_k \int_{\partial D} \psi d\sigma \quad \text{and} \quad \mathcal{S}_{D,n}^{(1),(2)}[\psi] := \int_{\partial D} G_n^{(1),(2)}(\cdot - \mathbf{y}) \psi(\mathbf{y}) d\sigma(\mathbf{y}). \quad (\text{A.5})$$

Similarly, the boundary integral operator is  $\mathcal{K}_D^{k,*}$  defined, for  $\mathbf{x} \in \partial D$ , by

$$\mathcal{K}_D^{k,*}[\psi](\mathbf{x}) = \int_{\partial D} \frac{\partial G_k(\mathbf{x}, \mathbf{y})}{\partial \nu_{\mathbf{x}}} \psi(\mathbf{y}) d\sigma(\mathbf{y}) = \mathcal{K}_D^*[\psi](\mathbf{x}) + \sum_{n=1}^{\infty} (k^{2n} \ln k) \mathcal{K}_{D,n}^{(1),*}[\psi](\mathbf{x}) + k^{2n} \mathcal{K}_{D,n}^{(2),*}[\psi](\mathbf{x}),$$

where the convergence holds in  $\mathcal{B}(L^2(\partial D))$ , and where we set

$$\mathcal{K}_{D,n}^{(1),(2),*}[\psi](x) = \int_{\partial D} \frac{\partial G_n^{(1),(2)}(\mathbf{x} - \mathbf{y})}{\partial \nu_{\mathbf{x}}} \psi(\mathbf{y}) d\sigma(\mathbf{y}).$$

**Lemma A.2.** *It holds that*

$$\mathcal{K}_{D,1}^{(1)}[\mathbb{1}_{\partial D}] = \frac{-|D|}{2\pi} \mathbb{1}_{\partial D} \quad \text{and} \quad \mathcal{K}_{D,1}^{(2)}[\mathbb{1}_{\partial D}](\mathbf{x}) = -\bar{\eta}_1 |D| \mathbb{1}_{\partial D}(\mathbf{x}) - \int_D G_0(\mathbf{x} - \mathbf{y}) d\mathbf{y}.$$

*Proof.* First, we have (notice that  $b_1 = -1/(8\pi)$ )

$$\mathcal{K}_{D,1}^{(1)}[\mathbb{1}_{\partial D}](\mathbf{x}) = \int_{\partial D} \frac{G_1^{(1)}(\mathbf{x} - \mathbf{y})}{\partial \nu_{\mathbf{y}}} d\sigma(\mathbf{y}) = \int_D \Delta_{\mathbf{y}} G_1^{(1)}(\mathbf{x} - \mathbf{y}) d\mathbf{y} = b_1 \int_D \Delta_{\mathbf{y}} |\mathbf{y} - \mathbf{x}|^2 d\mathbf{y} = \frac{-|D|}{2\pi}.$$

Then, using the equality

$$\forall \mathbf{x} \in \partial D, \quad \int_D |\mathbf{y} - \mathbf{x}|^2 \Delta \ln |\mathbf{y} - \mathbf{x}| d\mathbf{y} = 0,$$

we get

$$\begin{aligned} \mathcal{K}_{D,1}^{(2)}[\mathbb{1}_{\partial D}](\mathbf{x}) &= \int_{\partial D} \frac{\partial [|\mathbf{y} - \mathbf{x}|^2 (b_1 \ln |\mathbf{x} - \mathbf{y}| + \bar{c}_1)]}{\partial \nu_{\mathbf{y}}} d\sigma(\mathbf{y}) = \int_D \Delta_{\mathbf{y}} [|\mathbf{y} - \mathbf{x}|^2 (b_1 \ln |\mathbf{x} - \mathbf{y}| + \bar{c}_1)] d\mathbf{y} \\ &= 4\bar{c}_1 |D| + b_1 \int_D 4 \ln |\mathbf{x} - \mathbf{y}| d\mathbf{y} + b_1 \int_D 4 d\mathbf{y} = (4b_1 + 4\bar{c}_1) |D| - \int_D G_0(\mathbf{x} - \mathbf{y}) d\mathbf{y}. \end{aligned}$$

This completes the proof of the Lemma.  $\square$

## B The Minnaert resonance in two dimensions

In this section, we derive the Minnaert resonance for a single bubble in two dimensions using the same method we developed for the three-dimensional case. There are two main differences between the two-dimensional case and the three-dimensional case. First, the single layer potential  $\mathcal{S}_D$  may not be invertible from  $L^2(\partial D)$  to  $H^1(\partial D)$  in two dimensions, while this property always holds in three dimensions (see [1, 23] for more detail). Then, there is a logarithmic singularity in the asymptotic expansion of the single layer potential  $\mathcal{S}_D^k$  for small  $k$ . These create some difficulties which we address here.

Recall that

$$\mathcal{A}(\omega, \delta) = \begin{pmatrix} \mathcal{S}_D^{k_b} & -\mathcal{S}_D^k \\ -\frac{1}{2} + \mathcal{K}_D^{k_b,*} & -\delta(\frac{1}{2} + \mathcal{K}_D^{k,*}) \end{pmatrix},$$

where the boundary integral operators  $\mathcal{S}_D^k$  and  $\mathcal{K}_D^{k,*}$  are defined in Section A.2 together with their asymptotic expansions.

We denote by (recall that the operator  $\hat{\mathcal{S}}_D^k$  was defined in (A.5))

$$\mathcal{A}_0 := \begin{pmatrix} \hat{\mathcal{S}}_D^{k_b} & -\hat{\mathcal{S}}_D^k \\ -\frac{1}{2} + \mathcal{K}_D^* & 0 \end{pmatrix}. \tag{B.1}$$

It holds that  $\text{Ker}(-\frac{1}{2} + \mathcal{K}_D^*) = \text{Vect}\{\psi_0\}$ , where  $\psi_0$  is a real-valued function, normalized so that  $\int_{\partial D} \psi_0 d\sigma = 1$ . One can show that

$$\mathcal{S}_D[\psi_0] = -a \mathbb{1}_{\partial D} \tag{B.2}$$

for some  $a \geq 0$  (see [1, 23]). Actually, we can prove that if  $\mathcal{S}_D[\psi] \in \text{Vect}\{\mathbb{1}_{\partial D}\}$ , then  $\psi \in \text{Vect}\{\psi_0\}$ . If  $a = 0$ , then the operator  $\mathcal{S}_D$  is not invertible. We recall that, in two dimensions, the logarithm capacity of  $D$  is the positive number  $\text{Cap}_D := e^{-2\pi a}$ .

**Lemma B.1.** *For all  $k > 0$ , the operator  $\hat{\mathcal{S}}_D^k$  is invertible in  $\mathcal{B}(L^2(\partial D), H^1(\partial D))$ .*

*Proof.* Let us first show that  $\hat{\mathcal{S}}_D^k$  is injective. Assume that there exists  $\psi \in L^2(\partial D)$  so that

$$0 = \hat{\mathcal{S}}_D^k[\psi] = \mathcal{S}_D[\psi] + \eta_k(\psi, \mathbb{1}_{\partial D})\mathbb{1}_{\partial D}.$$

Then, since  $\mathcal{S}_D[\psi] \in \text{Vect}\{\mathbb{1}_{\partial D}\}$ , we deduce that  $\psi \in \text{Vect}\{\psi_0\}$  and we write  $\psi = \alpha\psi_0$ . The equation becomes

$$-a + \eta_k = 0, \quad \text{or equivalently} \quad \frac{\ln k}{2\pi} + \frac{1}{2\pi} \left( \gamma - \ln 2 - \frac{i\pi}{2} \right) = a.$$

Since the left-hand side always have a non null imaginary part, while the right-hand side is always real, this is not possible. The surjectivity of  $\hat{\mathcal{S}}_D^k$  follows from the fact that  $\hat{\mathcal{S}}_D^k$  is Fredholm with index zero. This completes the proof of the lemma.  $\square$

**Lemma B.2.** *We have  $\text{Ker}(\mathcal{A}_0) = \text{Vect}\{\Psi_0\}$  and  $\text{Ker}(\mathcal{A}_0^*) = \text{Vect}\{\Phi_0\}$  where*

$$\Psi_0 = \begin{pmatrix} (\eta_k - a)\psi_0 \\ (\eta_{k_b} - a)\psi_0 \end{pmatrix} \quad \text{and} \quad \Phi_0 = \begin{pmatrix} 0 \\ \mathbb{1}_{\partial D} \end{pmatrix}.$$

*Proof.* We first find the kernel space of  $\mathcal{A}_0$ . Assume that

$$\mathcal{A}_0 \begin{pmatrix} y_b \\ y \end{pmatrix} = \begin{pmatrix} \hat{\mathcal{S}}_D^{k_b}[y_b] - \hat{\mathcal{S}}_D^k[y] \\ (-\frac{1}{2} + \mathcal{K}_D^*)[y_b] \end{pmatrix} = 0 \quad \text{for some} \quad y_b, y \in L^2(\partial D).$$

We have

$$\mathcal{S}_D[y_b - y] + (\eta_{k_b}(y_b, \mathbb{1}_{\partial D}) - \eta_k(y, \mathbb{1}_{\partial D}))\mathbb{1}_{\partial D} = 0 \quad \text{and} \quad \left(-\frac{1}{2} + \mathcal{K}_D^*\right)[y_b] = 0.$$

From the second equation, we deduce that  $y_b$  is a multiple of  $\psi_0$ . We write  $y_b = \alpha\psi_0$  for some  $\alpha \in \mathbb{C}$ . The first equation becomes

$$\mathcal{S}_D[y] = (\eta_{k_b}\alpha - \eta_k(y, \mathbb{1}_{\partial D}) - a\alpha)\mathbb{1}_{\partial D},$$

and we deduce as before that  $y \in \text{Vect}\{\psi_0\}$ . We write  $y = \beta\psi_0$  for some  $\beta \in \mathbb{C}$ . We obtain that  $\beta(\eta_k - a) = \alpha(\eta_{k_b} - a)$ . This completes the proof of the first part of the Lemma. The second part of the Lemma follows from the fact that the operator  $\hat{\mathcal{S}}_D^k$  is injective.  $\square$

As in the three-dimensional case, we deduce that there exists a map  $\delta \mapsto \omega_0(\delta)$  of Minnaert resonances. Reasoning as before, we obtain the following theorem.

**Theorem B.1.** *In the quasi-static regime, there exist Minnaert resonances for a single bubble. Their leading order terms are given by the roots of*

$$\frac{k_b^2 |D|}{2\pi} \left( \ln(k \text{Cap}_D) + \gamma - \ln 2 - \frac{i\pi}{2} \right) + \delta = 0.$$

**Remark B.1.** *In the special case when  $D$  is a disk of radius  $R$ , we have  $|D| = \pi R^2$  and  $\text{Cap}_D = 1$ . Therefore, the Minnaert resonance in two dimensions is given by*

$$\frac{k_b^2 4\pi R^2}{2\pi} \left( \ln(k) + \gamma - \ln 2 - \frac{i\pi}{2} \right) + \delta = 0. \quad (\text{B.3})$$

*Proof of Theorem B.1.* As in Theorem 2.1, we can show that the resonances are the roots of

$$A(\omega, \delta) := \left( (\tilde{\mathcal{A}}_0 + \mathcal{B})^{-1} [\Phi_0], \Psi_0 \right) - 1 = 0. \quad (\text{B.4})$$

• **Asymptotic analysis of  $\mathcal{A}(\omega, \delta)$ .** We first study the operator  $\mathcal{A}(\omega, \delta)$ .

**Lemma B.3.** *In the space  $\mathcal{B}(\mathcal{H}, \mathcal{H}_1)$ , we have*

$$\mathcal{A}(\omega, \delta) := \mathcal{A}_0 + \mathcal{B}(\omega, \delta) = \mathcal{A}_0 + \omega^2 \ln \omega \mathcal{A}_{1,1,0} + \omega^2 \mathcal{A}_{1,2,0} + \delta \mathcal{A}_{0,1} + O(|\delta \omega^2 \ln \omega| + |\omega^4 \ln \omega|),$$

where

$$\mathcal{A}_{1,1,0} = \begin{pmatrix} v_b^{-2} \mathcal{S}_{D,1}^{(1)} & -v^{-2} \mathcal{S}_{D,1}^{(1)} \\ v_b^{-2} \mathcal{K}_{D,1}^{(1),*} & 0 \end{pmatrix}, \quad \mathcal{A}_{0,1} = \begin{pmatrix} 0 & 0 \\ 0 & -(\frac{1}{2} + \mathcal{K}_D^*) \end{pmatrix}.$$

and

$$\mathcal{A}_{1,2,0} = \begin{pmatrix} v_b^{-2} \left( -\ln v_b \mathcal{S}_{D,1}^{(1)} + \mathcal{S}_{D,1}^{(2)} \right) & -v^{-2} \left( -\ln v \mathcal{S}_{D,1}^{(1)} + \mathcal{S}_{D,1}^{(2)} \right) \\ v_b^{-2} \left( -\ln v_b \mathcal{K}_{D,1}^{(1)} + \mathcal{K}_{D,1}^{(2)} \right) & 0 \end{pmatrix},$$

We then define a projection  $\mathcal{P}_0$  by

$$\mathcal{P}_0[\Psi] := (\Psi, \Psi_0) \Phi_0,$$

and denote by

$$\tilde{\mathcal{A}}_0 = \mathcal{A}_0 + \mathcal{P}_0.$$

With the help of Lemma B.1, we can establish the following results.

**Lemma B.4.** *We have*

- (i) *The operator  $\tilde{\mathcal{A}}_0$  is a bijective operator in  $\mathcal{B}(\mathcal{H}, \mathcal{H}_1)$ . Moreover,  $\tilde{\mathcal{A}}_0[\Psi_0] = \|\Psi_0\|^2 \Phi_0$ ;*
- (ii) *Its adjoint  $\tilde{\mathcal{A}}_0^*$  is a bijective operator in  $\mathcal{B}(\mathcal{H}_1, \mathcal{H})$ . Moreover,  $\tilde{\mathcal{A}}_0^*[\Phi_0] = \|\Phi_0\|^2 \Psi_0$ .*

• **Strategy of the proof.**

By a direct calculation, we further have

$$\begin{aligned} \|\Psi_0\|^2 \|\Phi_0\|^2 A(\omega, \delta) &= -\omega^2 \ln \omega (\mathcal{A}_{1,1,0}[\Psi_0], \Phi_0) - \omega^2 (\mathcal{A}_{1,2,0}[\Psi_0], \Phi_0) \\ &\quad - \delta (\mathcal{A}_{0,1}[\Psi_0], \Phi_0) + O(|\omega^4 \ln \omega| + |\delta \omega^2 \ln \omega|). \end{aligned}$$

It is clear that

$$(\mathcal{A}_{1,1,0})^*[\Phi_0] = \begin{pmatrix} v_b^{-2} \mathcal{K}_{D,1}^{(1)}[\mathbb{1}_{\partial D}] \\ 0 \end{pmatrix} = \frac{-|D|}{2\pi v_b^2} \begin{pmatrix} \mathbb{1}_{\partial D} \\ 0 \end{pmatrix}, \quad \mathcal{A}_{0,1}[\Psi_0] = (a - \eta_{k_b}) \begin{pmatrix} 0 \\ \psi_0 \end{pmatrix},$$

and that

$$\begin{aligned} (\mathcal{A}_{1,2,0})^*[\Phi_0] &= \begin{pmatrix} v_b^{-2} \left( -\ln v_b \mathcal{K}_{D,1}^{(1)}[\mathbb{1}_{\partial D}] + \mathcal{K}_{D,1}^{(2)}[\mathbb{1}_{\partial D}] \right) \\ 0 \end{pmatrix} \\ &= \frac{|D|}{2\pi v_b^2} (\ln v_b - 2\pi\eta_1) \begin{pmatrix} \mathbb{1}_{\partial D} \\ 0 \end{pmatrix} - \frac{1}{v_b^2} \begin{pmatrix} \int_D G_0(\mathbf{x} - \mathbf{y}) d\mathbf{y} \\ 0 \end{pmatrix}, \end{aligned}$$

where we used Lemma A.2. It follows that

$$(\mathcal{A}_{1,1,0}[\Psi_0], \Phi_0) = \frac{(\eta_k - a)|D|}{2\pi v_b^2}, \quad (\mathcal{A}_{0,1}[\Psi_0], \Phi_0) = (a - \eta_{k_b}).$$

Moreover, using the fact that  $\mathcal{S}_D[\psi_0](\mathbf{x}) = -a$  for all  $\mathbf{x} \in D$ , so that

$$\int_{\partial D} \psi_0(\mathbf{x}) \int_D G_0(\mathbf{x} - \mathbf{y}) d\mathbf{y} d\sigma(\mathbf{x}) = \int_D d\mathbf{y} \int_{\partial D} G_0(\mathbf{x} - \mathbf{y}) \psi_0(\mathbf{y}) d\sigma(\mathbf{x}) = \int_D \mathcal{S}_D[\psi_0](\mathbf{y}) d\mathbf{y} = -a|D|,$$

we get

$$(\mathcal{A}_{1,2,0}[\Psi_0], \Phi_0) = \frac{(\eta_k - a)|D|}{2\pi v_b^2} (\ln v_b - 2\pi\eta_1 + 2\pi a).$$

Therefore, since  $\ln \omega - \ln v = \ln k$ , Equation (B.4) leads to

$$\omega^2 \frac{(\eta_k - a)|D|}{v_b^2} \left( \left[ \frac{\ln k_b}{2\pi} + \eta_1 \right] - a \right) - \delta(a - \eta_{k_b}) + O(|\omega^4 \ln \omega| + |\delta \omega^2 \ln \omega|) = 0.$$

The proof follows by noticing that the term in bra-ket is just  $\eta_{k_b}$ .  $\square$

## References

- [1] H. Ammari and H. Kang. *Polarization and moment tensors: with applications to inverse problems and effective medium theory*, volume 162. Springer Science & Business Media, 2007.
- [2] H. Ammari, H. Kang, and H. Lee. *Layer potential techniques in spectral analysis*, volume 153. American Mathematical Society Providence, 2009.
- [3] H. Ammari, P. Millien, M. Ruiz, and H. Zhang. Mathematical analysis of plasmonic nanoparticles: the scalar case. *arXiv preprint arXiv:1506.00866*, 2015.
- [4] H. Ammari and H. Zhang. A mathematical theory of super-resolution by using a system of sub-wavelength Helmholtz resonators. *Commun. in Math. Phys.*, 337(1):379–428, 2015.

- [5] H. Ammari and H. Zhang. Super-resolution in high-contrast media. *Proc. R. Soc. A*, 471(2178), 2015.
- [6] R.E. Caflisch, M.J. Miksis, G.C. Papanicolaou, and L. Ting. Effective equations for wave propagation in bubbly liquids. *J. Fluid Mech.*, 153:259–273, 1985.
- [7] R.E. Caflisch, M.J. Miksis, G.C. Papanicolaou, and L. Ting. Wave propagation in bubbly liquids at finite volume fraction. *J. Fluid Mech.*, 160:1–14, 1985.
- [8] D.C. Calvo, A.L. Thangawng, and C.N. Layman. Low-frequency resonance of an oblate spheroidal cavity in a soft elastic medium. *J. Acoust. Soc. Am.*, 132(1):EL1–EL7, 2012.
- [9] H. Cheng, W. Crutchfield, M. Doery, and L. Greengard. Fast, accurate integral equation methods for the analysis of photonic crystal fibers I: Theory. *Optics Express*, 12(16):3791–3805, 2004.
- [10] M. Devaud, Th. Hocquet, J.-C. Bacri, and V. Leroy. The Minnaert bubble: an acoustic approach. *Eur. J. Phys.*, 29(6):1263, 2008.
- [11] C. Feuillade. Scattering from collective modes of air bubbles in water and the physical mechanism of superresonances. *J. Acoust. Soc. Am.*, 98(2):1178–1190, 1995.
- [12] L.L. Foldy. The multiple scattering of waves. I. General theory of isotropic scattering by randomly distributed scatterers. *Phys. Rev.*, 67:107–119, 1945.
- [13] V. Galstyan, O.S. Pak, and H.A. Stone. A note on the breathing mode of an elastic sphere in Newtonian and complex fluids. *Phys. Fluids*, 27(3):032001, 2015.
- [14] I.C. Gohberg and E.I. Sigal. An operator generalization of the logarithmic residue theorem and the theorem of Rouché. *Sb. Math.*, 13(4):603–625, 1971.
- [15] P.A. Hwang and W.J. Teague. Low-frequency resonant scattering of bubble clouds. *J. Atmos. Oceanic Technol.*, 17(6):847–853, 2000.
- [16] S.G. Kargl. Effective medium approach to linear acoustics in bubbly liquids. *J. Acoust. Soc. Am.*, 111(1):168–173, 2002.
- [17] M. Lanoy, R. Pierrat, F. Lemoult, M. Fink, V. Leroy, and A. Tourin. Subwavelength focusing in bubbly media using broadband time reversal. *Phys. Rev. B*, 91(22):224202, 2015.
- [18] V. Leroy, A. Bretagne, M. Fink, H. Willaime, P. Tabeling, and A. Tourin. Design and characterization of bubble phononic crystals. *Appl. Phys. Lett.*, 95(17):171904, 2009.
- [19] V. Leroy, M. Devaud, and J.-C. Bacri. The air bubble: Experiments on an unusual harmonic oscillator. *Am. J. Phys.*, 70(10):1012–1019, 2002.
- [20] V. Leroy, A. Strybulevych, M.G. Scanlon, and J.H. Page. Transmission of ultrasound through a single layer of bubbles. *Eur. Phys. J. E*, 29(1):123–130, 2009.
- [21] M. Minnaert. XVI. On musical air-bubbles and the sounds of running water. *The London, Edinburgh, Dublin Philos. Mag. and J. of Sci.*, 16(104):235–248, 1933.

- [22] E.C. Titchmarsh. *Introduction to the Theory of Fourier Integrals (second edition)*. Oxford, Clarendon Press, 1948.
- [23] G. Verchota. Layer potentials and regularity for the Dirichlet problem for Laplace's equation in Lipschitz domains. *J. Funct. Anal.*, 59(3):572–611, 1984.